ISSN 1070-3284, Russian Journal of Coordination Chemistry, 2020, Vol. 46, No. 12, pp. 817–827. © Pleiades Publishing, Ltd., 2020.
Russian Text © The Author(s), 2020, published in Koordinatsionnaya Khimiya, 2020, Vol. 46, No. 12, pp. 738–748.

New Sterically Hindered Bis-*o*-Benzoquinones with Electron-Donor Bridging Groups and Related Binuclear Triphenylantimony(V) Catecholate Complexes

S. Yu. Bukhvalova[a], E. R. Zhiganshina[a], T. V. Astaf'eva[a], M. V. Arsenyev[a], E. V. Baranov[a], S. A. Chesnokov[a], and A. I. Poddel'sky[a, *]

[a] *Razuvaev Institute of Organometallic Chemistry, Russian Academy of Sciences, Nizhny Novgorod, Russia*
**e-mail: aip@iomc.ras.ru*

Received May 21, 2020; revised May 27, 2020; accepted June 8, 2020

Abstract—New bis-*o*-benzoquinones (3,5-Q)-6-CH_2O–$(CH_2)_n$–OCH_2-6-(3,5-Q) (n = 2 (L^1), 4 (L^2), and 6 (L^3)) and (3,5-Q)-6-$(CH_2OCH_2)_3$-6-(3,5-Q) (L^4) (3,5-Q is 3,5-di-*tert*-butyl-*o*-benzoquinone) with various diol spacers have been synthesized and characterized. The oxidative addition of $SbPh_3$ to these bis-*o*-benzoquinones affords binuclear triphenylantimony(V) bis(catecholate) complexes Ph_3Sb(3,5-Cat)-6-CH_2O–$(CH_2)_n$–OCH_2-6-(3,5-Cat)$SbPh_3$ (**I**–**III**, respectively) and Ph_3Sb(3,5-Cat)-6-$(CH_2OCH_2)_3$-6-(3,5-Cat)$SbPh_3$ (**IV**) (3,5-Cat is 3,5-di-*tert*-butyl catecholate). The molecular structures of quinones L^1–L^4 and bis(catecholate) complex **I** in the crystalline state were determined by X-ray diffraction analysis (CIF files CCDC nos. 1998601 (L^1), 1998602 (L^2), 1998603 (L^3), 1998604 (L^4), and 1998605 (**I** · *n*-pentane)).

Keywords: bis-*o*-benzoquinone, redox-active ligand, antimony, binuclear complex, X-ray diffraction analysis
DOI: 10.1134/S1070328420120027

INTRODUCTION

Organoantimony compounds are interesting objects of both coordination [1–8] and organic chemistry [9–14], since they have a high potential of application in medicine and pharmacology due to the antimicrobial, antiparasitic, and anticancer properties [15–19]. Researchers are interested in the antimony(V) complexes with redox-active ligands of the *o*-quinone type owing to the variety of structures formed by the antimony(V) compounds [20] and interesting chemical properties. For example, they are capable of reversibly adding molecular oxygen [21–26] and binding halide anions. They can be used as fluorescent sensors of fluoride anions [27–32], etc.

The coordination chemistry of bis-*o*-quinones is being intensively developed in the recent decades [33–41] but remains much less studied than the chemistry of the mononuclear analogues [42–45]. Synthesized by us 4,6-di-*tert*-butyl-2,3-dihydroxybenzaldehyde [46] and 4,6-di-*tert*-butyl-3-(methoxymethyl)catechol [47] are convenient structural blocks for the synthesis of sterically shielded bis-catechol and *o*-benzoquinones in high preparative yields. This study is a continuation of the cycle of works devoted to the synthesis and properties of oligomeric *o*-benzoquinones.

The synthesis and structures of sterically hindered bis-*o*-benzoquinones with flexible bridging groups based on diols and the synthesis of the related binuclear triphenylantimony(V) bis-catecholate complexes are described in this work.

EXPERIMENTAL

The solvents used were purified according to standard procedures [48]. Bis-catechols synthesized earlier [49] were oxidized to bis-*o*-benzoquinones using the procedure presented below.

Synthesis of (3,5-Q)-6-CH_2O–$(CH_2)_n$–OCH_2-6-(3,5-Q) (n = 2 (L^1), 4 (L^2), and 6 (L^3)) and (3,5-Q)-6-$(CH_2OCH_2)_3$-6-(3,5-Q) (L^4) (3,5-Q is 3,5-di-*tert*-butyl-*o*-benzoquinone). A solution of $K_3Fe(CN)_6$ (30 mmol) and KOH (12 mmol) in water (100 mL) was added to a solution of the corresponding bis-catechol) (3 mmol) in Et_2O (40 mL) with vigorous stirring. The reaction mixture was actively stirred for 45 min. Then the mixture was washed with water (3 × 100 mL), and the extract was dried over anhydrous sodium sulfate. The solvent was evaporated, and the residue of bis-*o*-benzoquinone was recrystallized from hexane (15 mL).

Ligand L^1, being 6,6'-(ethane-1,2-diylbis(oxymethylene))-bis-(3,5-di-*tert*-butyl-*o*-benzoquinone), was iso-

lated as yellow-green crystals (T_m = 148–150°C) in a yield of 1.35 g (85%).

For $C_{32}H_{46}O_6$

Anal. calcd., %	C, 72.97	H, 8.80
Found, %	C, 72.60	H, 8.90

IR (ν, cm^{-1}): 477 w, 518 w, 556 w, 573 w, 633 w, 640 w, 678 w, 695 w, 761 w, 787 w, 821 w, 843 w, 881 s, 923 w, 950 w, 964 w, 996 s, 1022 w, 1048 s, 1092 s, 1120 s, 1177 w, 1220 s, 1248 s, 1261 w, 1273 w, 1294 s, 1332 m, 1370 w, 1391 w, 1416 s, 1531 w, 1538 w, 1574 s, 1625 s, 1667 s, 1782 w, 1790 w, 2748 w, 2759 w, 3138 w, 3245 w, 3566 w.

^{1}H NMR ($CDCl_3$, 400 MHz), δ, ppm: 1.24 (s, 18H, *t*-Bu), 1.37 (s, 18H, *t*-Bu), 3.63 (s, 4H, O–CH_2–CH_2–O), 4.45 (s, 4H, CH_2–O), 7.07 (s, 2H, C_6H_1). ^{13}C NMR (100 MHz, $CDCl_3$), δ, ppm: 29.06, 30.03, 35.37, 38.66, 62.43, 70.03, 132.56, 137.21, 148.49, 159.69, 179.53, 182.36.

Ligand L^2, being 6,6'-(butane-1,4-diylbis(oxymethylene))-bis-(3,5-di-*tert*-butyl-*o*-benzoquinone), was isolated as red-green crystals (T_m = 93–95°C) in a yield of 1.37 g (83%).

For $C_{34}H_{50}O_6$

Anal. calcd., %	C, 73.61	H, 9.08
Found, %	C, 73.50	H, 9.24

IR (ν, cm^{-1}): 482 w, 516 w, 534 w, 578 w, 647 w, 679 w, 792 w, 843 w, 875 w, 925 w, 949 w, 984 s, 1011 s, 1028 w,1052 w, 1064 w, 1180 w, 1207 w, 1220 s, 1256 w, 1290 w, 1323 s, 1405 w, 1417 w, 1497 s, 1531 w, 1538 w, 1584 s, 1632 s, 1668 s, 2752 s, 2881 w, 3247 w, 3263 w, 3851 w.

^{1}H NMR (400 MHz, $CDCl_3$), δ, ppm: 1.24 (s, 18H, *t*-Bu), 1.38 (s, 18H, *t*-Bu), 1.62 (m, 4H, O–CH_2–C<u>H</u>$_2$-C<u>H</u>$_2$–CH_2–O), 3.46 (m, 4H, O–C<u>H</u>$_2$–CH_2–CH_2–C<u>H</u>$_2$–O), 4.38 (s, 4H, CH_2–O), 7.08 (s, 2H, C_6H_1). ^{13}C NMR (100 MHz, $CDCl_3$), δ, ppm: 26.51, 29.08, 30.04, 35.38, 38.64, 62.16, 70.67, 132.66, 137.19, 148.49, 159.53, 179.50, 182.34.

Ligand L^3, being 6,6'-(hexane-1,6-butane-1,4-diyl-bis(oxymethylene))-bis-(3,5-di-*tert*-butyl-*o*-benzoquinone), was isolated as green crystals (T_m = 116–118°C) in a yield of 1.37 g (78%).

For $C_{36}H_{54}O_6$

Anal. calcd., %	C, 74.19	H, 9.34
Found, %	C, 74.47	H, 9.58

IR (ν, cm^{-1}): 482 w, 516 w, 527 w, 550 w, 578 w, 643 w, 657 w, 697 w, 792 w, 818 w, 840 w, 876 w, 896 w, 925 w, 949 w, 979 w, 1001 w, 1013 s, 1034 w,1052 w, 1069 w, 1139 w, 1163 w, 1185 w, 1222 w, 1254 s, 1291 w, 1323 s, 1406 w, 1419 w, 1497 s, 1533 w, 1539 w, 1584 s, 1630 s, 1669 s, 1846 w, 1980 w, 2753 s, 2881 w, 3250 w, 3257 w, 3854 w.

^{1}H NMR (400 MHz, $CDCl_3$), δ, ppm: 1.24 (s, 18H, *t*-Bu), 1.33 (m, 4H, O–CH_2–CH_2–C<u>H</u>$_2$–C<u>H</u>$_2$–CH_2–CH_2–O), 1.39 (s, 18H, *t*-Bu), 1.56 (m, 4H, O–CH_2–C<u>H</u>$_2$–CH_2–CH_2–C<u>H</u>$_2$–CH_2–O), 3.44 (t, ^3J(H,H) = 6.6 Hz, 4H, O–C<u>H</u>$_2$–CH_2–CH_2–CH_2–CH_2–C<u>H</u>$_2$–O), 4.38 (s, 4H, CH_2–O), 7.08 (s, 2H, C_6H_1). ^{13}C NMR (100 MHz, $CDCl_3$), δ, ppm: 26.03, 29.08, 29.65, 30.00, 35.37, 38.66, 62.14, 70.95, 132.70, 137.21, 148.46, 159.54, 179.50, 182.34.

Ligand L^4, being 6,6'-((oxy-bis(ethane-2,1-diyl))-bis-(oxymethylene)-bis-(3,5-di-*tert*-butyl-*o*-benzoquinone), was isolated as dark green crystals (T_m = 88–90°C) in a yield of 1.40 g (83%).

For $C_{34}H_{50}O_7$

Anal. calcd., %	C, 71.55	H, 8.83
Found, %	C, 71.32	H, 8.49

IR (ν, cm^{-1}): 478 w, 516 w, 551 w, 575 w, 633 w, 639 w, 679 w, 707 w, 731 w, 788 w, 817 w, 838 w, 871 s, 906 w, 926 w, 936 w, 981 w, 1012 w, 1052 s, 1105 w, 1128 w, 1139 w, 1166 w, 1175 w, 1219 w, 1254 s, 1292 w, 1320 s, 1348 w, 1409 s, 1420 w, 1495 s, 1531 w, 1537 w, 1582 s, 1629 s, 1666 s, 1789 w, 1915 w, 1998 w, 2749 s, 2759 w, 3253 w, 3258 w, 3647 w.

^{1}H NMR (400 MHz, $CDCl_3$), δ, ppm: 1.23 (s, 18H, *t*-Bu), 1.38 (s, 18H, *t*-Bu), 3.61 (s, 8H, O–CH_2–CH_2–O), 4.46 (s, 4H, CH_2–O), 7.07 (s, 2H, C_6H_1). ^{13}C NMR (100 MHz, $CDCl_3$), δ, ppm: 29.05, 29.98, 35.36, 38.66, 62.46, 69.98, 70.34, 132.47, 137.20, 148.49, 159.77, 179.46, 182.30.

Synthesis of Ph_3Sb(3,5-Cat)-6-CH_2O–$(CH_2)_n$–OCH_2-6-(3,5-Cat)$SbPh_3$ (n = 2 (I), 4 (II), and 6 (III)) and Ph_3Sb(3,5-Cat)-6-$(CH_2OCH_2)_3$-6-(3,5-Cat)-$SbPh_3$ (IV) (3,5-Cat is 3,5-di-*tert*-butyl-catecholate) was carried out in evacuated ampules in the absence of oxygen and moisture using a described procedure [50]. Solutions of triphenylantimony (0.176 g, 0.5 mmol, 15 mL of toluene) and the corresponding bis-*o*-benzoquinone (0.25 mmol, 15 mL of toluene) were mixed at room temperature. The green color of the solutions gradually disappeared during the reaction course, and the solution became yellow after the end of the reaction. The complexes were light yellow powders stable in air.

Complex **I** is 3,3'-(ethane-1,2-diyl-bis(oxymethylene)-bis-((4,6-di-*tert*-butylcatecholato)triphenylantimony(V)). Triphenylantimony (134 mg, 0.38 mmol) and quinone L^1 (100 mg, 0.19 mmol) were used. After the solutions was concentrated and kept at room temperature for 24 h, the formed precipitate was filtered

off and dried in vacuo. The yield of the product as a yellow finely crystalline powder was 198 mg (85%).

For $C_{68}H_{76}O_6Sb_2$

Anal. calcd., %	C, 66.25	H, 6.21	Sb, 19.75
Found, %	C, 66.64	H, 6.35	Sb, 19.54

IR (ν, cm^{-1}): 3071 w, 3055 w, 2953 s, 2923 s, 2853 s, 1708 w, 1638 w, 1631 w, 1594 w, 1578 w, 1552 w, 1463 s, 1434 s, 1413 s, 1406 s, 1413 s, 1378 s, 1365 w, 1332 w, 1317 w, 1293 s, 1260 m, 1241 s, 1211 w, 1178 w, 1160 w, 1098 m, 1090 m, 1073 m, 1059 m, 1031 w, 1005 m, 997 m, 962 s, 924 m, 873 w, 863 w, 792 w, 785 w, 748 s, 732 s, 693 s, 656 w, 625 m, 594 w, 564 w, 533 w, 513 w, 454 s.

^{1}H NMR (400 MHz, $CDCl_3$), δ, ppm: 1.44 (s, 18H, *t*-Bu), 1.45 (s, 18H, *t*-Bu), 3.89 (s, 4H, O–CH_2–CH_2–O), 4.94 (s, 4H, Ar–CH_2–O), 6.76 (s, 2H, arom. C_6H_1), 7.37–7.47 (s, 18H, arom. $SbPh_3$), 7.78–7.84 (m, 12H, arom. $SbPh_3$). ^{13}C NMR (100 MHz, $CDCl_3$), δ, ppm: 29.62, 32.76, 34.71, 35.91, 67.05, 69.99, 112.66, 118.45, 129.06, 131.01, 132.55, 135.18, 137.55, 138.03, 142.97, 148.03.

Complex **II** is 3,3'-(butane-1,4-diyl-bis(oxymethylene))-bis-((4,6-di-*tert*-butylcatecholato)triphenylantimony(V)). Triphenylantimony (127 mg, 0.36 mmol) and quinone L^2 (100 mg, 0.18 mmol) were used. The yield of the product as a light yellow powder was 180 mg (79%).

For $C_{70}H_{80}O_6Sb_2$

Anal. calcd., %	C, 66.68	H, 6.40	Sb, 19.31
Found, %	C, 66.83	H, 6.52	Sb, 19.14

IR (ν, cm^{-1}): 3051 w, 2954 s, 2924 s, 2854 s, 2727 w, 1594 w, 1578 w, 1552 w, 1462 s, 1434 m, 1411 m, 1405 m, 1377 m, 1366 m, 1352 m, 1315 w, 1291 m, 1262 m, 1241 m, 1212 w, 1192 w, 1181 w, 1156 w, 1094 m, 1063 m, 1023 w, 1008 w, 997 m, 961 m, 871 w, 860 w, 783 w, 760 w, 748 m, 734 s, 693 s, 666 w, 656 w, 624 m, 564 w, 532 w, 514 w, 492 m.

^{1}H NMR (400 MHz, $CDCl_3$), δ, ppm: 1.40 (s, 18H, *t*-Bu), 1.41 (s, 18H, *t*-Bu), 1.75 (m, 4H, O–CH_2–C<u>H</u>$_2$–C<u>H</u>$_2$–CH_2–O), 3.61 (t, ^3J(H,H) = 5.6 Hz, 4H, O–C<u>H</u>$_2$–CH_2–CH_2–C<u>H</u>$_2$–O), 4.81 (s, 4H, Ar–CH_2–O), 6.71 (s, 2H, arom. C_6H_1), 7.37–7.43 (m, 18H, arom. $SbPh_3$), 7.74–7.81 (m, 12H, arom. $SbPh_3$). ^{13}C NMR (100 MHz, $CDCl_3$), δ, ppm: 27.16, 29.64, 32.70, 34.69, 35.88, 66.79, 70.98, 112.58, 118.64, 129.04, 131.01, 132.42, 135.21, 137.46, 138.07, 142.99, 148.00.

Complex **III** is 3,3'-(hexane-1,6-diyl-bis(oxy-methylene))-bis-((4,6-di-*tert*-butylcatecholato)triphenylantimony(V)). Triphenylantimony (120 mg, 0.34 mmol) and quinone L^3 (100 mg, 0,17 mmol) were used. The yield of the product as a yellow powder was 190 mg (87%).

For $C_{72}H_{84}O_6Sb_2$

Anal. calcd., %	C, 67.09	H, 6.57	Sb, 18.89
Found, %	C, 67.30	H, 6.70	Sb, 18.61

IR (ν, cm^{-1}): 3579 w, 3057 w, 3043 w, 2954 s, 2924 s, 2854 s, 1961 w, 1908 w, 1886 w, 1819 w, 1773 w, 1764 w, 1644 m, 1590 m, 1578 m, 1549 m, 1479 m, 1462 s, 1430 s, 1416 s, 1385 m, 1377 m, 1362 m, 1333 m, 1305 w, 1289 s, 1258 m, 1248 m, 1240 m, 1210 m, 1184 m, 1157 w, 1081 s, 1075 s, 1052 s, 1024 w, 1000 s, 961 m, 950 m, 912 m, 875 m, 861 m, 818 w, 792 w, 765 w, 748 m, 737 s, 696 s, 679 w, 662 w, 626 w, 613 w, 511 w, 482 w, 456 m.

^{1}H NMR (400 MHz, $CDCl_3$), δ, ppm: 1.36 (m, 4H, O–CH_2–CH_2–C<u>H</u>$_2$–C<u>H</u>$_2$–CH_2–CH_2–O), 1.40 (s, 18H, *t*-Bu), 1.41 (s, 18H, *t*-Bu), 1.63 (m, 4H, O–CH_2–C<u>H</u>$_2$–CH_2–CH_2–C<u>H</u>$_2$–CH_2–O), 3.58 (t, ^3J(H,H) = 6.8 Hz, 4H, O–C<u>H</u>$_2$–CH_2–CH_2–CH_2–CH_2–C<u>H</u>$_2$–O), 4.81 (s, 4H, Ar-CH_2-O), 6.71 (s, 2H, arom. C_6H_1), 7.39–7.46 (m, 18H, arom. $SbPh_3$), 7.77–7.82 (m, 12H, arom. $SbPh_3$). ^{13}C NMR (100 MHz, $CDCl_3$), δ, ppm: 26.51, 29.63, 30.11, 32.69, 34.69, 35.89, 66.72, 71.14, 112.72, 118.57, 129.03, 131.01, 132.43, 135.24, 137.39, 138.13, 143.10, 147.81.

Complex **IV** is 3,3'-(oxy-bis(ethane-2,1-diyloxymethylene))-bis-((4,6-di-*tert*-butylcatecholato)tri-phenylantimony(V)). Triphenylantimony (123 mg, 0.35 mmol) and quinone L^4 (100 mg, 0.175 mmol) were used. The yield of the product as a light yellow powder was 181 mg (81%).

For $C_{70}H_{80}O_7Sb_2$

Anal. calcd., %	C, 65.84	H, 6.32	Sb, 19.07
Found, %	C, 65.97	H, 6.40	Sb, 18.95

IR (ν, cm^{-1}): 3070 w, 3055 w, 2954 s, 2925 s, 2725 w, 1463 s, 1435 m, 1411 s, 1403 s, 1377 s, 1304 w, 1288 m, 1262 m, 1242 w, 1210 w, 1160 w, 1104 w, 1078 m, 1063 m, 1022 w, 997 m, 961 w, 863 w, 787 w, 782 w, 748 w, 733 m, 693 m, 622 w, 564 w, 533 w, 511 w, 440 s.

^{1}H NMR (400 MHz, $CDCl_3$), δ, ppm: 1.41 (s, 18H, *t*-Bu), 1.42 (s, 18H, *t*-Bu), 3.65 (t, ^3J(H,H) = 5.4 Hz, 4H, (Ar–CH_2–O–CH_2–C<u>H</u>$_2$)$_2$O), 3.76 (t, ^3J(H,H) = 5.4 Hz, 4H, (Ar–CH_2–O–C<u>H</u>$_2$–CH_2)$_2$O), 4.92 (s, 4H, Ar–CH_2–O), 6.73 (s, 2H, arom. C_6H_1), 7.39–7.48 (m, 18H, arom. $SbPh_3$), 7.76–7.83 (m, 12H, arom. $SbPh_3$). ^{13}C NMR (100 MHz, $CDCl_3$), δ, ppm: 29.60, 32.69, 34.68, 35.89, 66.98, 69.73, 70.66, 112.65, 118.29, 129.05, 131.01, 132.53, 135.18, 137.58, 138.08, 142.94, 148.01.

^{1}H and ^{13}C NMR spectra were recorded on Bruker-Avance HD-400 spectrometer with a frequency of 400 MHz using tetramethylsilane as the internal stan-

dard and $CDCl_3$ as the solvent. IR spectra were recorded on an FSN-1201 FT-IR spectrometer in a range of 400–4000 cm^{-1} in Nujol. Elemental analyses to C, H, and Sb were carried out by the pyrolytic method with the gravimetric end.

The crystals of compounds L^1–L^4 suitable for X-ray diffraction analysis were obtained by slow crystallization from a solution in *n*-hexane, and the crystals of complex **I** were crystallized from pentane in the form of solvate **I** · *n*-pentane.

X-ray diffraction analysis (XRD). Diffraction data on the crystals of compounds L^1–L^4 and **I** were collected on a Bruker D8 Quest single-crystal X-ray diffractometer at 100 K. Experimental sets of intensities (MoK_α radiation, ω and φ scan modes) were integrated using the SAINT program [51]. The structures were determined by the "dual-space" method using the SHELXT program [52] and refined by full-matrix least squares for F^2_{hkl} in the anisotropic approximation for all non-hydrogen atoms using the SHELXTL program package [53]. Hydrogen atoms were placed in the geometrically calculated positions and refined isotropically. An absorption correction was applied using the SADABS program [54]. One of the *o*-quinone fragments in L^4 and one phenyl ring in each Ph_3Sb fragment, as well as the $-CH_2OCH_2CH_2OCH_2-$ bridge of bis(catecholate) in compound **I**, were disordered over two positions. The molecular structures were drawn using the OLEX2 program [55]. The solvate pentane molecule disordered over two common positions was found in the crystal of compound **I** (ratio 1 : 1 to the antimony complex). The crystallographic data and structure refinement parameters for compounds L^1–L^4 and **I** are presented in Table 1.

The structural data were deposited with the Cambridge Crystallographic Data Centre (CIF files CCDC nos. 1998601 (L^1), 1998602 (L^2), 1998603 (L^3), 1998604 (L^4), and 1998605 (**I** · *n*-pentane); deposit@ccdc.cam.ac.uk; www: http://www.ccdc.cam.ac.uk).

RESULTS AND DISCUSSION

The oxidation of bis-catechols, which were synthesized earlier via the interesterification of 4,6-di-*tert*-butyl-3-(methoxymethyl)catechol by diols (ethane-1,2-diol, butane-1,2-diol, hexane-1,2-diol, and diethylene glycol), using potassium ferricyanide in an alkaline medium (Scheme 1) affords in high yields the corresponding bis-*o*-benzoquinones L^1–L^4 with the flexible CH_2O–R–OCH_2 bridging groups based on diols. Binuclear triphenylantimony(V) complexes **I**–**IV** were synthesized via the oxidative addition of bis-*o*-benzoquinones to triphenylantimony (Scheme 1). This method for the synthesis of the complexes facilitates the isolation of the target compounds, since secondary reaction products, which cannot be avoided in the synthesis of the complexes by the substitution of catechols by triphenylantimony(V) dibromide, are absent in the most cases.

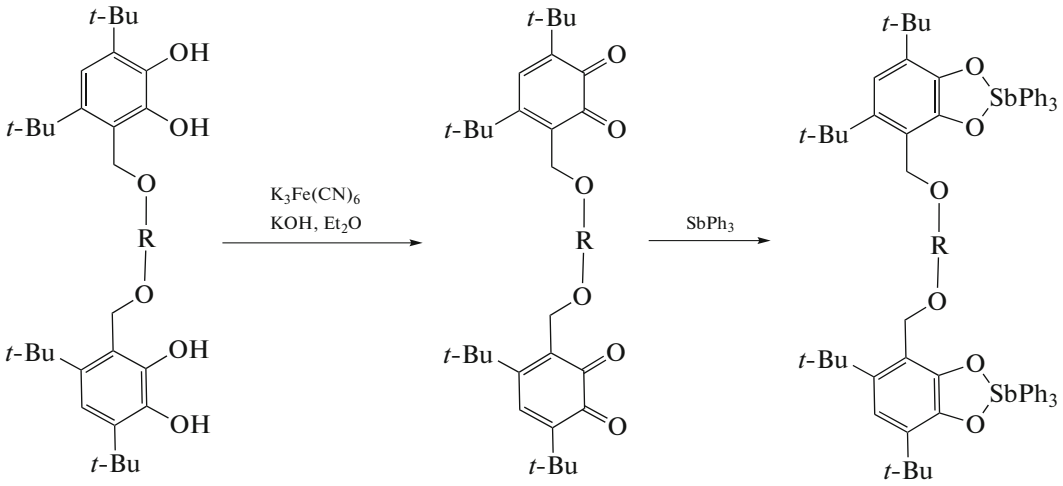

L^1: R = $(CH_2)_2$, 85%
L^2: R = $(CH_2)_4$, 83%
L^3: R = $(CH_2)_6$, 78%
L^4: R = $CH_2CH_2OCH_2CH_2$, 83%

I, 85%
II, 79%
III, 87%
IV, 81%

Scheme 1.

Table 1. Selected crystallographic data and structure refinement parameters for compounds L^1–L^4 and **I**

Parameter	L^1	L^2	L^3	L^4	**I** · *n*-pentane
Empirical formula	$C_{32}H_{46}O_6$	$C_{34}H_{50}O_6$	$C_{36}H_{54}O_6$	$C_{34}H_{50}O_7$	$C_{73}H_{88}O_6Sb_2$
FW	526.69	554.74	582.79	570.74	1304.93
T, K	100(2)	100(2)	100(2)	100(2)	100(2)
Crystal system	Triclinic	Monoclinic	Monoclinic	Triclinic	Triclinic
Space group	$P\bar{1}$	*C*2/*c*	*C*2/*c*	$P\bar{1}$	$P\bar{1}$
a, Å	9.8257(7)	24.6406(15)	25.692(14)	9.5388(4)	13.1643(4)
b, Å	10.8671(8)	11.7979(7)	12.149(7)	9.6584(4)	14.9533(5)
c, Å	14.0510(9)	12.2934(7)	11.919(6)	18.9126(8)	19.1987(6)
α, deg	100.406(3)	90	90	84.952(2)	68.5910(11)
β, deg	90.075(3)	117.2994(9)	116.315(7)	87.143(2)	71.1952(11)
γ, deg	90.420(4)	90	90	68.646(2)	72.1616(11)
V, Å^3	1475.60(18)	3175.7(3)	3335(3)	1616.20(12)	3253.46(18)
Z	2	4	4	2	2
ρ_{calc}, g/cm^3	1.185	1.160	1.161	1.173	1.332
μ, mm^{-1}	0.080	0.078	0.077	0.080	0.881
F(000)	572	1208	1272	620	1352
$2\theta_{max}$, deg	50.00	56.00	46.43	60.33	58.00
Number of measured/ independent reflections	6882/4950	16600/3835	10095/2352	24305/9561	49462/17210
R_{int}	0.0377	0.0302	0.1303	0.0313	0.0269
Number of refined parameters	356	187	196	499	812
R_1, wR_2 ($I > 2\sigma(I)$)	0.0634, 0.1550	0.0383, 0.0994	0.0694, 0.1351	0.0519, 0.1221	0.0304, 0.0674
R_1, wR_2 (for all data)	0.0805, 0.1773	0.0460, 0.1029	0.1147, 0.1493	0.0795, 0.1356	0.0441, 0.0710
GOOF for F^2	1.068	1.052	1.071	1.018	1.007
Residual electron density (max/min), e/Å^3	0.290/–0.335	0.397/–0.192	0.237/–0.250	0.346/–0.282	0.915/–0.516

Bis-*o*-benzoquinones L^1–L^4 and bis-catecholate complexes **I**–**IV** were isolated in the individual state and characterized by IR spectroscopy, NMR spectroscopy, and elemental analysis. The single crystals suitable for XRD were grown for compounds L^1–L^4 and **I**, and their structures were confirmed by the XRD method.

According to the ^{1}H NMR data, the molecules considered are symmetric in the solution: singlets of the *tert*-butyl fragments are observed at 1.23–1.24 and 1.37–1.39 ppm for bis-*o*-quinones (at 1.40–1.44 and 1.41–1.45 ppm for triphenylantimony catecholates), singlets of the OCH_2 groups at the six-membered carbon ring are observed at 4.38–4.46 ppm for bis-*o*-quinones and 4.81–4.94 ppm for triphenylantimony catecholates, singlets of the protons in the quinone rings of compounds L^1–L^4 appear at 7.07–7.08 ppm, and singlets of the corresponding protons in the aromatic rings of the catecholate ligands in complexes **I–IV** are observed at 6.71–6.76 ppm. The data of ^{13}C NMR spectroscopy also confirm that the quinone fragments of compounds L^1–L^4 are equivalent, as those of the catecholate fragments in complexes **I**–**IV**: two signals of the carbon atoms of the carbonyl groups in the spectra of bis-*o*-quinones L^1–L^4 are observed at 178–183 ppm, which are absent from the spectra of complexes **I**–**IV**. However, the signals of the carbon atoms in a range of 100–130 ppm corresponding to the carbon atoms in the aromatic rings are observed in these spectra.

The IR spectra of bis-*o*-quinones exhibit the characteristic bands of stretching vibrations of the double C=O bonds in a range of 1650–1680 cm^{-1}. These bands are absent from the spectra of complexes **I**–**IV**, but a set of bands is observed at 1170–1300 cm^{-1} due to stretching vibrations of the ordinary C–O bonds of the catecholate ligands, which are absent from the spectra of bis-*o*-quinones. The IR spectra of complexes **I**–**IV**

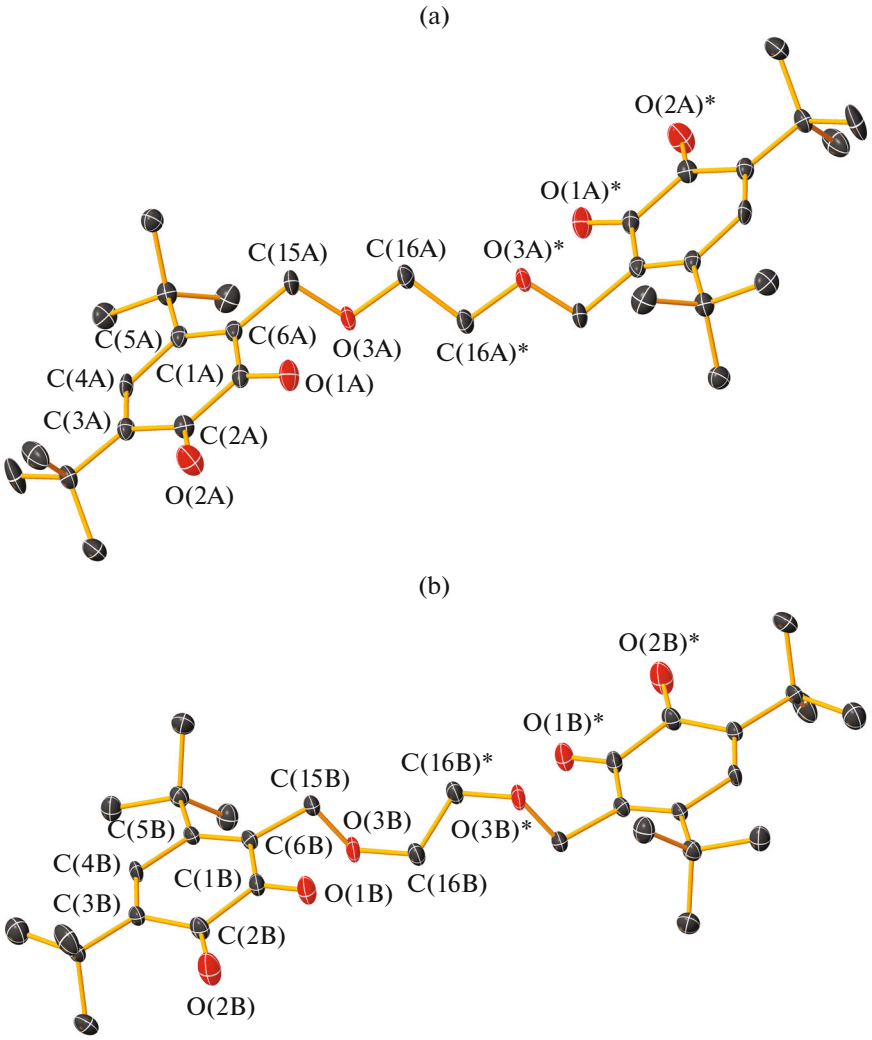

Fig. 1. Molecular structures of molecules (a) **A** and (b) **B** of bis-*o*-benzoquinone L^1. Thermal ellipsoids of 50% probability. Hydrogen atoms are omitted. Selected bond lengths and torsion angle in L^1A: C(1)–O(1) 1.224(4), C(2)–O(2) 1.203(4), C(1)–C(2) 1.549(4), C(2)–C(3) 1.480(4), C(3)–C(4) 1.347(5), C(4)–C(5) 1.478(4), C(5)–C(6) 1.364(4), C(6)–C(1) 1.472(5), C(6)–C(15) 1.505(4), C(15)–O(3) 1.423(4), O(3)–C(16) 1.422(3), C(16)–C(16)* 1.500(7); in L^1B: C(1)–O(1) 1.210(4), C(2)–O(2) 1.208(4), C(1)–C(2) 1.549(4), C(2)–C(3) 1.471(5), C(3)–C(4) 1.325(5), C(4)–C(5) 1.490(4), C(5)–C(6) 1.355(5), C(6)–C(1) 1.466(5), C(6)–C(15) 1.515(4), C(15)–O(3) 1.446(4), O(3)–C(16) 1.424(4), C(16)–C(16)* 1.520(6) Å; O(1)C(1)C(2)O(2) 2.6(5)° (L^1A) and 6.3(5)° (L^1B).

contain bands in a range of 620–650 cm^{-1} and those of Sb–O at 440–470 cm^{-1} corresponding to stretching vibrations of the Sb–C_{Ph} bond, which are absent from the spectra of the corresponding bis-*o*-quinones.

The molecular structures of compounds L^1–L^4 and **I** in the crystalline state are shown in Figs. 1–5, respectively. The presence of the flexible bridge between the quinone (in L^1–L^4) and catecholate fragments (in **I**–**IV**) makes it possible to expect both the unfolded (when the distance between the fragments at the end of the bridge is maximum) and compact (when the distance between the fragments is considerably less than the maximum one) forms of the molecule in the crystal.

It was found by the XRD study that the crystalline cell of bis-*o*-quinone L^1 contained two independent molecules (Figs. 1a and 1b) differed in geometry of the $-CH_2OCH_2CH_2OCH_2-$ bridge between the *o*-quinone fragments. Both these molecules are symmetric with the inversion center at the middle of the C(16A)–C(16A)* and C(16B)–C(16B)* bonds, respectively. Unlike compound L^1, in compounds L^2–L^4 the crystalline cell contains only one independent molecule. The molecules of compounds L^2 and L^3 (Figs. 2 and 3) are symmetric with the inversion center at the middle of the C(17)–C(17)* and C(18)–C(18)* bonds, respectively. The molecule of compound L^4 (Fig. 4) has no symmetry. The geometric characteristics of the redox-active fragments in compounds L^1–L^4 corre-

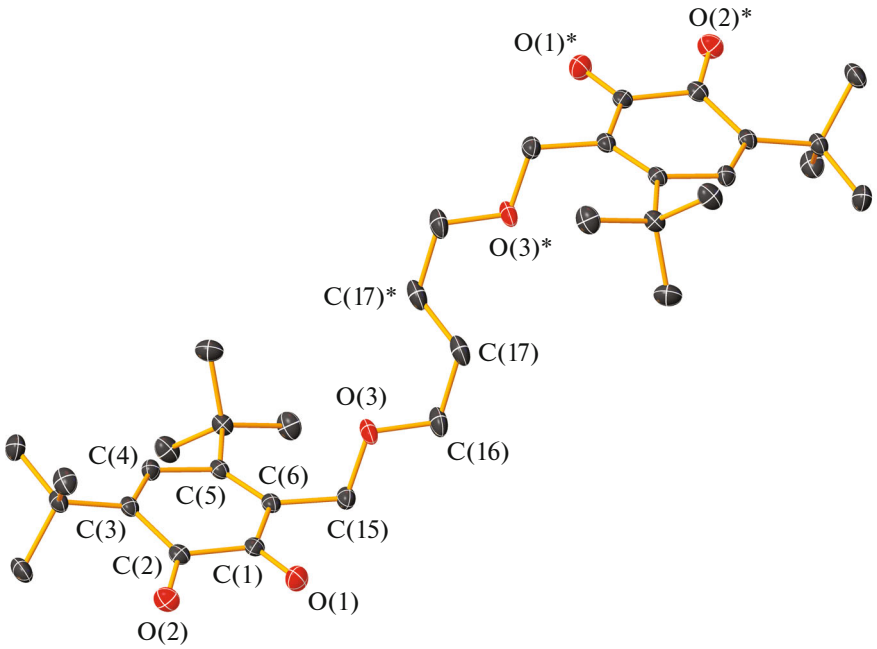

Fig. 2. Molecular structure of bis-*o*-benzoquinone L^2. Thermal ellipsoids of 50% probability. Hydrogen atoms are omitted. Selected bond lengths and torsion angle: C(1)–O(1) 1.2153(13), C(2)–O(2) 1.2168(12), C(1)–C(2) 1.5547(13), C(2)–C(3) 1.4713(14), C(3)–C(4) 1.3451(14), C(4)–C(5) 1.4853(13), C(5)–C(6) 1.3598(14), C(6)–C(1) 1.4768(14), C(6)–C(15) 1.5100(13), C(15)–O(3) 1.4313(12), O(3)–C(16) 1.4270(12), C(16)–C(17) 1.5174(16), C(17)–C(17)* 1.528(2) Å and O(1)C(1)C(2)O(2) 11.86(13)°.

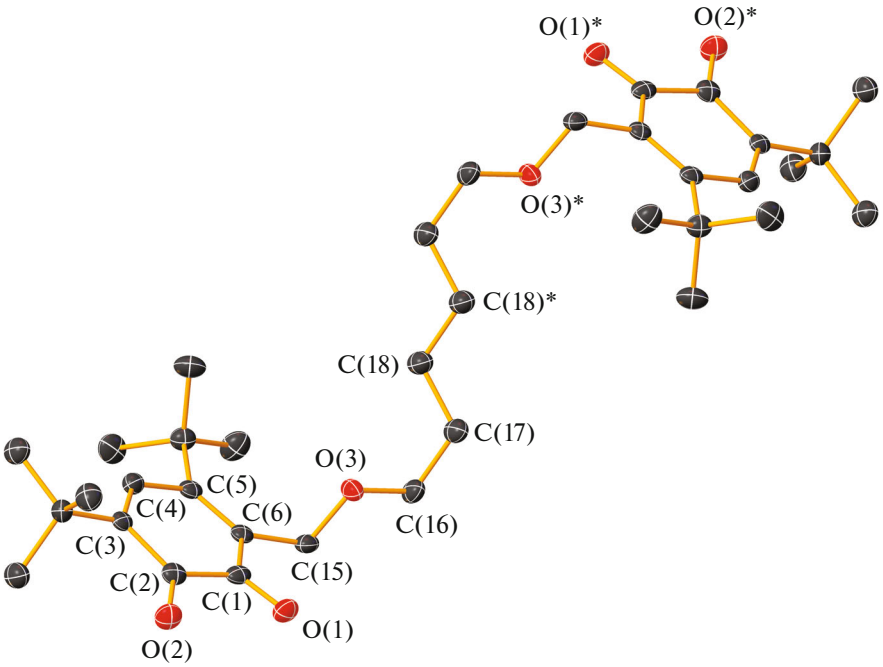

Fig. 3. Molecular structure of bis-*o*-benzoquinone L^3. Thermal ellipsoids of 50% probability. Hydrogen atoms are omitted. Selected bond lengths and torsion angle: C(1)–O(1) 1.210(4), C(2)–O(2) 1.205(4), C(1)–C(2) 1.517(5), C(2)–C(3) 1.461(5), C(3)–C(4) 1.337(5), C(4)–C(5) 1.470(5), C(5)–C(6) 1.342(5), C(6)–C(1) 1.458(5), C(6)–C(15) 1.476(5), C(15)–O(3) 1.409(4), O(3)–C(16) 1.421(4), C(16)–C(17) 1.489(5), C(17)–C(18) 1.513(5), C(18)–C(18)* 1.493(7) Å and O(1)C(1)C(2)O(2) 12.7(5)°.

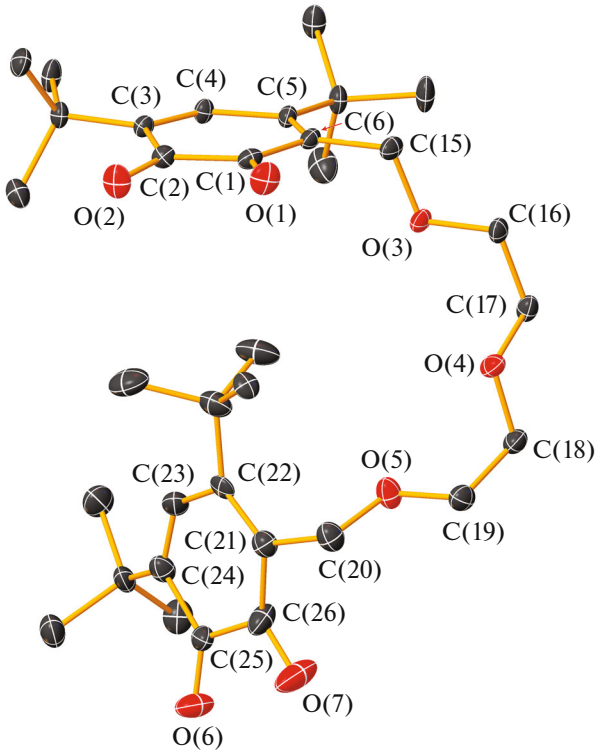

Fig. 4. Molecular structure of bis-*o*-benzoquinone L^4. Thermal ellipsoids of 50% probability. Hydrogen atoms are omitted. Selected bond lengths and torsion angle: C(1)–O(1) 1.2164(14), C(2)–O(2) 1.2145(14), C(1)–C(2) 1.5479(16), C(2)–C(3) 1.4731(15), C(3)–C(4) 1.3459(15), C(4)–C(5) 1.4822(15), C(5)–C(6) 1.3641(16), C(6)–C(1) 1.4751(16), C(6)–C(15) 1.5061(15), C(15)–O(3) 1.4256(14), O(3)–C(16) 1.4228(13), C(16)–C(17) 1.5002(17), C(17)–O(4) 1.4122(14), O(4)–C(18) 1.4204(15), C(18)–C(19) 1.4981(18), C(19)–O(5) 1.4248(15), O(5)–C(20) 1.4216(15), C(20)–C(21) 1.5092(18), C(21)–C(22) 1.335(5), C(22)–C(23) 1.478(5), C(23)–C(24) 1.304(4), C(24)–C(25) 1.490(3), C(25)–C(26) 1.565(3), C(26)–C(21) 1.4668(19), O(6)–C(25) 1.223(3), O(7)–C(26) 1.2135(17) Å and O(1)C(1)C(2)O(2) 6.5(2)°, O(6)C(25)C(26)O(7) 1.9(4)°.

spond to the values characteristic of *o*-quinones [46, 47, 50, 56] (C–O (1.203(4)–1.224(4) Å) and C–C in the six-membered rings (1.304(4)–1.364(4) and 1.458(5)–1.565(3) Å) (Table 1). The quinone fragments in compounds L^1–L^4 are nonplanar: the C(1)–C(6) atoms shift from the plane by 0.004–0.189 Å, and the O(1) and O(2) atoms shift from the plane by 0.053–0.451 Å. The distances between the quinone fragments (the centroids between the carbon atoms of the quinone ring and oxygen atoms of the corresponding carbonyl groups were taken for the calculation) increase regularly with the elongation of the bridge and are equal to 10.22(1) Å (**A**) and 10.67(1) Å (**B**), 12.35(1) Å, 13.44(1) Å for compounds L^1–L^3, respectively. Unlike compounds L^1–L^3, the molecule of compound L^4 exists in the folded conformation due to the intramolecular π...H interaction between the quinone ring C(1–6) and hydrogen atom of the *t*-Bu substituent at the C(22) atom. The dihedral angle between the *o*-quinone planes is 81.6°, and the distance between the centers of the quinone fragments is 7.83(2) Å.

Unlike the initial L^1 in the molecule of which the *o*-quinone fragments are remote from each other at the maximum distance, the bis-catecholate ligand in the molecule of complex **I** (Fig. 5) has the folded conformation similarly to the molecule of compound L^4. The distance between the centers of the catecholate fragments is 8.24(1) Å, which is significantly shorter than that in L^1. Probably, this is due to the intramolecular π–π and H–π interactions between $Ph^{C(45)}...Ph^{C(63)}$ and $Ph^{C(45)}$–H...$Cat^{C(19–24)}$, $Ph^{C(63)}$–H...$Cat^{C(1–6)}$, respectively. The oxygen atoms O(1,2) and O(5,6) of the catecholate fragments are oppositely directed, and the angle of turn is ~164°. The dihedral angle between the O(1,2)C(1–6) and O(5,6)C(19–24) planes is ~54°.

Both antimony atoms are characterized by a distorted tetragonal pyramidal geometry: for Sb(1) and Sb(2) $\tau = 0.03$ and 0.17, respectively ($\tau = 0$ for an ideal tetragonal pyramid and $\tau = 1$ for an ideal trigonal bipyramid [57]). In the metallocycle containing the Sb(1) atom, the O(1) and O(2) oxygen atoms of the catecholate fragment and the C(33) and C(39) carbon atoms of two phenyl groups lie in the base of the pyramid and the C(45) carbon atom of the third phenyl group occupies the apical position. The Sb–C apical bond is shorter than the equatorial bonds by 0.046 and 0.049 Å, respectively. The antimony atom shifts from the plane of the pyramid base by 0.529 Å, and the angles between the equatorial and axial substituents range from 99.1(2)° to 110.0(2)°. The Sb–O(Cat) bonds are insignificantly differentiated, and the Sb(1)–O(1) bond is shorter than Sb(1)–O(2) by 0.026 Å. In the metallocycle containing the Sb(2) atom, the O(5) and O(6) oxygen atoms of the catecholate fragment and carbon atoms C(51) and C(57) of two phenyl groups lie in the base of the pyramid, and the C(63) carbon atom of the third phenyl group occupies the apical position. The apical Sb–C bond is shorter than the equatorial bonds by 0.033 and 0.038 Å. The antimony atom shifts from the plane of the pyramid base by 0.496 Å, and the angles between the equatorial and axial substituents lie in the range 96.77(7)°–108.01(8)°. The Sb(2)–O(6) bond is shorter than Sb(2)–O(5) by 0.027 Å.

In both cases, the metallocycles are nonplanar. The inflection angles along the O...O line with respect to the catecholate ligand plane is 15.0° for the cycle containing the Sb(1) atom and 17.5° for the cycle containing Sb(2).

The geometric characteristics of the redox-active fragments C–O (1.357(2)–1.369(2) Å and C–C in the six-membered rings (1.390(3)–1.418(3) Å) corre-

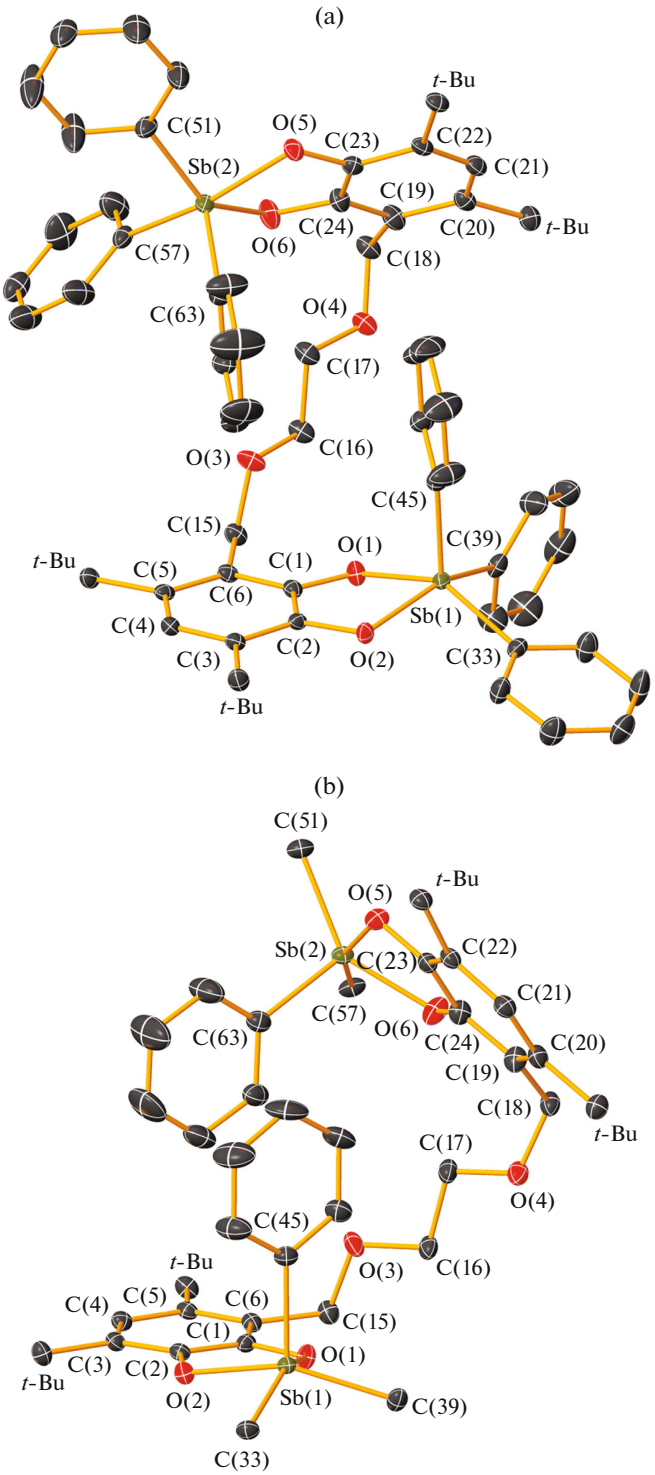

Fig. 5. Molecular structure of triphenylantimony(V) bis-catecholate **I** (a, b) from different sides. Thermal ellipsoids of 50% probability, hydrogen atoms are omitted, and *t*-Bu are *tert*-butyl substituents. The carbon atoms of four phenyl groups (except for the C(33), C(39), C(51), and C(57) atoms bound to the central antimony atom) are omitted in Fig. 5b. Selected bond lengths and bond angles: Sb(1)–O(1) 2.0196(13), Sb(1)–O(2) 2.0453(13), Sb(1)–C(33) 2.1416(19), Sb(1)–C(39) 2.139(2), Sb(1)–C(45) 2.093(4), Sb(2)–O(5) 2.0417(13), Sb(2)–O(6) 2.0150(15), Sb(2)–C(51) 2.135(2), Sb(2)–C(57) 2.140(4), Sb(2)–C(63) 2.102(2), O(1)–C(1) 1.359(2), O(2)–C(2) 1.364(2), O(3)–C(16) 1.430(2), O(3)–C(15) 1.435(2), O(4)–C(17) 1.423(2), O(4)–C(18) 1.430(2), O(5)–C(23) 1.357(2), O(6)–C(24) 1.369(2), C(1)–C(2) 1.397(3), C(1)–C(6) 1.392(3), C(2)–C(3) 1.393(3), C(3)–C(4) 1.403(3), C(4)–C(5) 1.398(3), C(5)–C(6) 1.408(3), C(6)–C(15) 1.507(3), C(16)–C(17) 1.510(3), C(18)–C(19) 1.526(3), C(19)–C(24) 1.400(3), C(19)–C(20) 1.418(3), C(20)–C(21) 1.390(3), C(21)–C(22) 1.398(3), C(22)–C(23) 1.392(3), C(23)–C(24) 1.396(3) Å and O(1)Sb(1)C(33) 147.74(7)°, O(2)Sb(1)C(39) 149.67(7)°, O(5)Sb(2)C(57) 156.9(3)°, O(6)Sb(2)C(51) 142.98(7)°.

spond to the values characteristic of the catecholate complexes [50, 58–66].

Thus, new bis-*o*-benzoquinones with the bridging groups $CH_2–O(CH_2)_nO–CH_2–$ (n = 2, 4, and 6) and $–CH_2–O(CH_2)_2O(CH_2)_2O–CH_2–$ between the quinone fragments were synthesized and characterized. New binuclear triphenylantimony(V) catecholate complexes were synthesized on the basis of these bis-*o*-benzoquinones. The molecular structures of all bis-*o*-benzoquinones and one binuclear triphenylantimony(V) bis-catecholate complex $Ph_3Sb(3,5\text{-Cat})\text{-}6\text{-}CH_2O–(CH_2)_2–OCH_2\text{-}6\text{-}(3,5\text{-Cat})SbPh_3$ in the crystalline state were determined by the XRD method. Unlike the initial bis-*o*-benzoquinone, the triphenylantimony bis-catecholate molecule exists in the folded conformation, and the oxygen atoms of the catecholate fragments are directed oppositely due to the intramolecular π–π and H–π interactions.

ACKNOWLEDGMENTS

The studies were carried out using the equipment of the Analytical Center for Collective Use at the Razuvaev Institute of Organometallic Chemistry (Russian Academy of Sciences) in terms of the federal target program "Investigation and Developments on Priority Directions of the Scientific Technological Complex of Russia for 2014–2020" (unique project identifier RFMEFI62120X0040).

FUNDING

The synthesis of bis-*o*-benzoquinones was supported by the Russian Foundation for Basic Research (project no. 19-33-90263). The synthesis and study of the antimony(V) catecholate complexes were in the accordance with state assignment of the Razuvaev Institute of Organometallic Chemistry (Russian Academy of Sciences).

CONFLICT OF INTEREST

The authors declare that they have no conflicts of interest.

REFERENCES

1. Levason, W. and Reid, G., *Comprehensive Coordination Chemistry II*, McCleverty, J.A. and Meyer, T.J., Eds., Elsevier, 2003, p. 465.
2. Jones, C., *Coord. Chem. Rev.*, 2001, vol. 215, p. 151.
3. Shiragami, T., Matsumoto, J., Inoue, H., and Yasuda, M., *J. Photochem. Photobiol.*, 2005, vol. 6, p. 227.
4. Lo, Y.-H. and Gabbaï, F.P., *Organometalics*, 2018, vol. 37, no. 15, p. 2500.
5. You, D., Yang, H., Sen, S., and Gabbaï, F.P., *J. Am. Chem. Soc.*, 2018, vol. 140, no. 30, p. 9644.
6. Jones, J.S. and Gabbaï, F.P., *Chem.-Eur. J.*, 2017, vol. 23, no. 5, p. 1136.
7. Jones, J.S. and Gabbaï, F.P., *Acc. Chem. Rev.*, 2016, vol. 49, p. 857.
8. Liu, R.-C., Ma, Y.-Q., Yu, L., et al., *Appl. Organomet. Chem.*, 2003, vol. 17, p. 662.
9. You, D., Smith, J.E., Sen, S., and Gabbaï, F.P., *Organometallics*, 2020. https://doi.org/10.1021/acs.organomet.0c00193
10. Sen, S., Ke, I.Sh., and Gabbaï, F.P., *Organometallics*, 2017, vol. 36, no. 21, p. 4224.
11. You, D. and Gabbaï, F.P., *J. Am. Chem. Soc.*, 2017, vol. 139, no. 20, p. 6843.
12. Pan, B. and Gabbaï, F.P., *J. Am. Chem. Soc.*, 2014, vol. 136, no. 27, p. 9564.
13. Huang, Y., *Acc. Chem. Res.*, 1992, vol. 25, p. 182.
14. Finet, J.P., *Ligand Coupling Reactions with Heteroatomic Compounds*, New York: Pergamon, 1998.
15. Hadjikakou, S.K., Ozturk, I.I., Banti, C.N., et al., *J. Inorg. Biochem.*, 2015, vol. 153, p. 293.
16. Reglinski, J., *The Chemistry of Arsenic, Antimony and Bismuth,* Norman, N.C., Ed., London: Blackie, 1998.
17. Wormser, U. and Nir, I., *Chemistry of Organic Arsenic, Antimony and Bismuth Compounds*, Patai, S., Ed., New York: Wiley, 1994, p. 715.
18. Ge, R. and Sun, H., *Acc. Chem. Res.*, 2007, vol. 40, p. 267.
19. Sharma, P., Perez, D., Cabrera, A., et al., *Acta Pharmacol. Sin.*, 2008, vol. 29, no. 8, p. 881.
20. Poddel'sky, A.I., *Antimony: Characteristics, Compounds and Applications*, Razeghi, M., Ed., New York: Nova Science, 2012, p. 271.
21. Abakumov, G.A., Poddel'sky, A.I., Grunova, E.V., et al., *Angew. Chem., Int. Ed. Engl.*, 2005, vol. 44, p. 2767.
22. Cherkasov, V.K., Abakumov, G.A., Grunova, E.V., et al., *Chem.-Eur. J.*, 2006, vol. 12, no. 14, p. 3916.
23. Poddel'sky, A.I., Smolyaninov, I.V., Kurskii, Yu.A., et al., *J. Organomet. Chem.*, 2010, vol. 695, no. 8, p. 1215.
24. Poddel'sky, A.I., Kurskii, Yu.A., Piskunov, A.V., et al., *Appl. Organomet. Chem.*, 2011, vol. 25, no. 3, p. 180.
25. Fukin, G.K., Baranov, E.V., Jelsch, C., et al., *J. Phys. Chem. A*, 2011, vol. 115, no. 29, p. 8271.
26. Fukin, G.K., Baranov, E.V., Poddel'sky, A.I., et al., *Chem. Phys. Chem.*, 2012, vol. 13, no. 17, p. 3773.
27. Kumar, A., Yang, M., Kim, M., et al., *Organometallics*, 2017, vol. 36, no. 24, p. 4901.
28. Christianson, A.M. Gabbaï, F.P., et al., *Organometallics*, 2017, vol. 36, no. 16, p. 3013.
29. Christianson, A.M., Rivard, E., and Gabbaï, F.P., *Organometallics*, 2017, vol. 36, no. 14, p. 2670.
30. Hirai, M. and Gabbaï, F.P., *Angew. Chem., Int. Ed. Engl.*, 2015, vol. 54, p. 1205.
31. Chen, C.-H. and Gabbaï, F.P., *Angew. Chem., Int. Ed. Engl.*, 2017, vol. 56, p. 1799.
32. Wade, C.R., Ke, I.S., and Gabbaï, F.P., *Angew. Chem., Int. Ed. Engl.*, 2012, vol. 51, p. 478.
33. Abakumov, G.A., Nevodchikov, V.I., Druzhkov, N.O., et al., *Russ. Chem. Bull.*, 1997, vol. 46, no. 4, p. 771. https://doi.org/10.1007/BF02495211
34. Bencini, A., Daul, C.A., Dei, A., et al., *Inorg. Chem.*, 2001, vol. 40, no. 7, p. 1582.

35. Shultz, D.A., *Comment. Inorg. Chem*., 2002, vol. 23, p. 1.
36. Piskunov, A.V., Cherkasov, V.K., Druzhkov, N.O., et al., *Russ. Chem. Bull.*, 2005, vol. 54, no. 7, p. 1627. https://doi.org/10.1007/s11172-006-0014-8
37. Poddel'sky, A.I., Piskunov, A.V., Druzhkov, N.O., et al., *Z. Anorg. Allg. Chem*., 2009, vol. 635, p. 2563.
38. Arsenyev, M.V., Astaf'eva, T.V., Baranov, E.V., et al., *Mendeleev Commun.*, 2018, vol. 28, p. 76.
39. Kuropatov, V.A., Klementieva, S.V., Poddel'sky, A.I., et al., *Russ. Chem. Bull.*, 2010, vol. 59, p. 1698. https://doi.org/10.1007/s11172-010-0299-5
40. Poddel'sky, A.I., Smolyaninov, I.V., Vavilina, N.N., et al., *Russ. J. Coord. Chem*., 2012, vol. 38, p. 284. https://doi.org/10.1134/S1070328412040094
41. Arsen'ev, M.V., Okhlopkova, L.S., Poddel'skii, A.I., et al., *Russ. J. Coord. Chem*., 2018, vol. 44, p. 162. https://doi.org/10.1134/S1070328418020021
42. Pierpont, C.G., *Coord. Chem. Rev.*, 2001, vols. 216–217, p. 99.
43. Pierpont, C.G., *Coord. Chem. Rev.*, 2001, vols. 219–221, p. 415.
44. Zanello, P. and Corsini, M., *Coord. Chem. Rev.*, 2006, vol. 250, p. 2000.
45. Bubnov, M.P., Piskunov, A.V., Zolotukhin, A.A., et al., *Russ. J. Coord. Chem*., 2020, vol. 46, no. 4, p. 224. https://doi.org/10.1134/S107032842003001X
46. Arsenyev, M.V., Baranov, E.V., Shurygina, M.P., et al., *Mendeleev Commun.*, 2016, vol. 26, p. 552.
47. Arsenyev, M.V., Baranov, E.V., Fedorov, A.Yu., et al., *Mendeleev Commun.*, 2015, vol. 25, p. 312.
48. Gordon, A. and Ford, R., *The Chemist's Companion: A Handbook of Practical Data, Techniques, and References*, New York: Wiley, 1972.
49. Zhiganshina, E.R., Arsenyev, M.V., Shavyrin, A.S., et al., *Mendeleev Commun.*, 2019, vol. 29, p. 91.
50. Poddel'sky, A.I., Arsenyev, M.V., Astaf'eva, T.V., et al., *J. Organomet. Chem.*, 2017, vol. 835, p. 17.
51. *SAINT. Data Reduction and Correction Program*, *Version 8.38A*, Madison: Bruker AXS, 2017.
52. Sheldrick, G.M., *Acta Crystallogr., Sect. A: Found. Adv.*, 2015, vol. 71, p. 3.
53. Sheldrick, G.M., *SHELXTL. Version 6.14. Structure Determination Software Suite*, Madison: Bruker AXS, 2003.
54. Sheldrick, G.M., *SADABS. Version 2012/1. Bruker/Siemens Area Detector Absorption Correction Program*, Madison: Bruker AXS, 2012.
55. Dolomanov, O.V., Bourhis, L.J., Gildea, R.J., et al., *J. Appl. Crystallogr.*, 2009, vol. 42, p. 339.
56. Abakumov, G.A., Cherkasov, V.K., Kocherova, T.N., et al., *Russ. Chem. Bull.*, 2007, vol. 56, p. 1849. https://doi.org/10.1007/s11172-007-0287-6
57. Addison, A.W., Rao, T.N., Reedijk, J., et al., *J. Chem. Soc., Dalton Trans.*, 1984, p. 1349.
58. Brown, S.N., *Inorg. Chem*., 2012, vol. 51, p. 1251.
59. Poddel'sky, A.I., Baranov, E.V., Fukin, G.K., et al., *J. Organomet. Chem.*, 2013, vol. 733, p. 44.
60. Poddel'sky, A.I., Smolyaninov, I.V., Berberova, N.T., et al., *J. Organomet. Chem.*, 2015, vols. 789–790, p. 8.
61. Poddel'sky, A.I., Smolyaninov, I.V., Fukin, G.K., et al., *J. Organomet. Chem.*, 2016, vol. 824, p. 1.
62. Poddel'sky, A.I., Astaf'eva, T.V., Smolyaninov, I.V., et al., *J. Organomet. Chem.*, 2018, vol. 873, p. 57.
63. Poddel'sky, A.I., Smolyaninov, I.V., Fukin, G.K., et al., *J. Organomet. Chem.*, 2018, vol. 867, p. 238.
64. Okhlopkova, L.S., Poddel'sky, A.I., Smolyaninov, I.V., et al., *J. Organomet. Chem.*, 2019, vol. 897, p. 32.
65. Okhlopkova, L.S., Smolyaninov, I.V., Baranov, E.V., and Poddel'sky, A.I., *Russ. J. Coord. Chem*., 2020, vol. 46, p. 466. https://doi.org/10.1134/S1070328420060081
66. Poddel'skii, A.I., Okhlopkova, L.S., Meshcheryakova, I.N., et al., *Russ. J. Coord. Chem*., 2019, vol. 45, p. 133. https://doi.org/10.1134/S1070328419010093

Translated by E. Yablonskaya